3-10-2010

Rubidium Recycling in a High Intensity Short Duration Pulsed Alkali Laser

Wooddy S. Miller

RUBIDIUM RECYCLING IN A HIGH INTENSITY SHORT DURATION PULSED ALKALI LASER

THESIS

Wooddy S. Miller, Second Lieutenant, USAF

AFIT/GAP/ENP/10-M11

DEPARTMENT OF THE AIR FORCE
AIR UNIVERSITY

AIR FORCE INSTITUTE OF TECHNOLOGY

Wright-Patterson Air Force Base, Ohio

The views expressed in this thesis are those of the author and do not reflect the official policy or position of the United States Air Force, Department of Defense, or the U.S. Government.

AFIT/GAP/ENP/10-M11

RUBIDIUM RECYCLING IN A HIGH INTENSITY SHORT DURATION PULSED ALKALI LASER

THESIS

Presented to the Faculty

Department of Engineering Physics

Graduate School of Engineering and Management

Air Force Institute of Technology

Air University

Air Education and Training Command

In Partial Fulfillment of the Requirements for the

Degree of Master of Science in Applied Physics

Wooddy S. Miller, BS

Second Lieutenant, USAF

March 2010

AFIT/GAP/ENP/10-M11

RUBIDIUM RECYCLING IN A HIGH INTENSITY SHORT DURATION PULSED ALKALI LASER

Wooddy S. Miller, BS

Second Lieutenant, USAF

Approved:

//SIGNED//	_____
Lt Col Jeremy C. Holtgrave (Chairman)	Date
//SIGNED//	_____
Glen P. Perram Ph.D. (Member)	Date
//SIGNED//	_____
Lt Col Michael R. Hawks (Member)	Date

Abstract

Laser induced fluorescence was used to study how pump pulse duration and alkali recycle time effects maximum power output in a Diode Pumped Alkali Laser (DPAL) system. A high intensity short pulsed pump source was used to excited rubidium atoms inside a DPAL-type laser. The maximum output power of the laser showed a strong dependence upon the temporal width of the pump pulse in addition to the input pump intensity. A linear relationship was observed between the maximum output power and the pulse width due to the effective lifetime of the excited state, defined as the time it takes for the alkali to be excited to the $^2P_{3/2}$, relax down to the $^2P_{1/2}$ state, and finally lase. This effective lifetime, calculated to be 0.139 ns, allowed for a calculation of the number of times each alkali atom in the pump volume could be used for lasing during a pulse. The number of recycles ranged from approximately 15 during the shorter 2 ns pulses up to 50+ times during the 7-8 ns pulses. The maximum output of the system scaled linearly with the number of cycles available.

Acknowledgments

I would like to express my sincere appreciation to my faculty advisor, Lt Col Jeremy Holtgrave, and project advisor, Dr. Glen Perram, for their guidance and support throughout the course of this thesis effort. The insight and experience was certainly appreciated. I would, also, like to thank Maj Cliff Sulham and Mr. Greg Smith for the support, knowledge, and expertise provided to me in this endeavor. Lastly, I would like to thank my wife for her support and understanding.

Wooddy S. Miller

Table of Contents

Page

List of Figures

Page

List of Tables

Page

RUBIDIUM RECYCLING IN A HIGH INTENSITY

SHORT DURATION PULSED ALKALI LASER

I. Introduction

Research Motivation

Over the last several decades lasers have come to the forefront of modern military technology. Lasers are used in a variety of applications from range finding to imaging to weapons applications. As the public tolerance for collateral damage lessens higher accuracy weapons become ever more important with laser guided conventional munitions and even laser weapons. The most recent use of lasers on the battlefield is not imaging or even as a guidance system, but as weapons unto themselves. Two of the current systems in development for military use are the Airborne Laser (ABL) and the Advanced Tactical Laser (ATL). The ABL is housed in a modified Boeing 747 and is designed to heat the skin of a ballistic missile during its boost phase in order to cause a structural failure that subsequently destroys the missile.[1] The ATL is designed for more of a tactical role using a smaller system than the ABL, designed to fit on an AC-130, and is less powerful.[2] Targets for the ATL would most likely include vehicles and small structures at a much closer range than the typical ABL target.

These weapon systems use a chemical laser known as a Chemical Oxygen Iodine Laser (COIL). In the COIL a mixture of chlorine and peroxide react to form an excited oxygen molecule and some byproducts. The excited oxygen is then used to collisionally excite iodine which lases down at the 1.315 micron wavelength.[3] The COIL system has a

variety of drawbacks for military use including thermal management issues, a limited number of shots due to the chemical reactions necessary, and a long logistical trail to deliver the hazardous chemicals to the battlefront where they are needed.[3] Research is ongoing into alternative laser types that do not have these drawbacks.

Alternative lasers that show the most promise for weapon systems include Diode Pumped Alkali Lasers (DPALs), the Joint High Power Solid State Laser (JHPSSL)[4], and the Free Electron Laser (FEL). Each of these systems is still in the development stage and research is ongoing to push these systems towards weapons grade powers. The DPAL laser is an optically pumped gas-phase laser with excellent heat management. On the other hand the FEL has favorable wavelength tuneability and power selectivity while the solid state lasers are easily pumped by electricity and relatively inexpensive to build. Currently the Air Force Institute of Technology performs a substantial amount of research on DPAL systems.

Since the DPAL is a relatively new laser system it is not completely understood. Research is ongoing in multiple areas to characterize all the facets of this new system. Areas of particular interest include laser efficiency and scaling of DPALs to higher and higher powers, mode volume overlap, spin-orbit relaxation rates, temperature dependence, pressure broadening, pulsed versus Continuous Wave (CW) systems and others. This research deals with investigating how alkali atoms are recycled through the system while using a short (2-8 ns) pulsed source. The reusability of each alkali atom in pulsed systems, which offer the highest intensities, directly impacts the maximum power available from the system and is therefore of interest in the scaling of these systems.

II. Background

Energy Level Diagram

The Diode Pumped Alkali Laser (DPAL) is a three-level laser employing an alkali vapor as the gain medium. A diagram representing a DPAL system first demonstrated by Konefal *et al*. can be seen in Figure 1.[5]

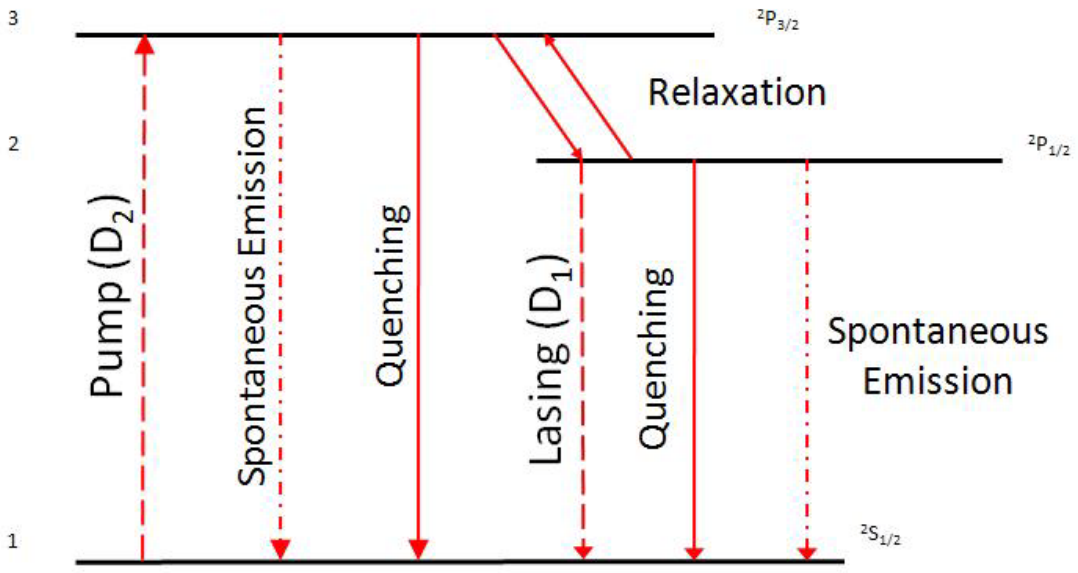

Figure 1. Three-Level DPAL Representation. This representation of a DPAL system shows optical transitions with dashed arrows and mechanical transitions with solid arrows.

As can be seen from the diagram of the three-level laser system there are a number of processes that need to be taken into account. Each will be detailed next.

The D_2 transition occurs between the ground $^2S_{1/2}$ state and the excited $^2P_{3/2}$ state and its wavelength for the various alkalis is listed in Table 1. The DPAL is pumped via this transition moving population from the $^2S_{1/2}$ to the $^2P_{3/2}$ state. This can be

troublesome as the unbroadened, or natural, absorption linewidth of this transition is on the order of hundredths of a GHz[6] while most diode pump sources are quite broadband on the order of tens of GHz. To overcome this difference in pump versus absorption linewidths, a broadening gas is mixed with the alkali vapor that broadens the absorption profile. This will be discussed in depth later. The $^2P_{3/2}$ state is partially depleted by two processes known as quenching and spontaneous emission down to the ground state. While there is ongoing research into the quenching rate, the lifetime of the spontaneous emission is approximately 26.2 ns for rubidium and 30.4 ns for cesium as listed in Tables 2 and 4 below. That means that in order to preserve efficiency and create a population inversion in the $^2P_{1/2}$ state the excited alkalis must be moved out of the $^2P_{3/2}$ state down to the $^2P_{1/2}$ state at a rate much higher than the combined spontaneous emission and quenching rates of these two states. This occurs through a process called either spin-orbit (SO) relaxation[6] or fine-structure (FS) mixing.[7]

SO relaxation requires collisions either with other alkali atoms or with a small molecule in the form of a relaxing gas. Through collisions with each other and a relaxing gas inserted into the system, the effective transfer of excited atoms can take place between the two fine structure states. Furthermore the relaxing gas must move the atoms at a rate much greater than the combined spontaneous emission and quenching rates of the $^2P_{3/2}$ state and the combined spontaneous and quenching emission of the $^2P_{1/2}$ state.[6] Also possible along this transition is the excitation of atoms back up to the $^2P_{3/2}$ state through collisions. This transition back up to the $^2P_{3/2}$ state from the $^2P_{1/2}$ state is small

and is taken into account by subtracting its rate from the $^2P_{3/2}$ to $^2P_{1/2}$ relaxation rate to give an overall relaxation rate for the system.

Once a population inversion in the $^2P_{1/2}$ state is achieved through the process described above, lasing can occur via the D_1 transition from the $^2P_{1/2}$ to the $^2S_{1/2}$ state. The wavelength of this transition is listed for the various alkalis in Table 1. However, the $^2P_{1/2}$ state is depleted by two competing process; spontaneous emission and quenching. The spontaneous emission lifetime of atoms in the $^2P_{1/2}$ state is approximately 27.7 ns for rubidium and 34.8 ns for cesium as listed in Tables 3 and 5 which become important when looking at population inversion for lasing. The quenching rates for the $^2P_{1/2}$ states of rubidium and cesium will be discussed shortly.

Alkalis

The alkali metals, in particular, rubidium, cesium, and potassium, display a number of positive features that make their use as a DPAL gain medium desirable. As discussed previously their single valence electron leads to a simple three-level system described above. Other features include relatively small quantum defects and ease of handling. The quantum defect is defined as the difference in energy between the $^2P_{3/2}$ and the $^2P_{1/2}$ states and is listed in Table 1 for the various alkalis.[6] Though having the smallest quantum defect is typically desirable the closeness of the energy states producing the defect makes it difficult to pump one transition and not the other. This typically leads to choosing an alkali that has enough separation between the D_1 and D_2 lines to be easily used in an experiment yet still has a relatively small quantum defect.

Table 1. Alkali D_1 and D_2 Transition Wavelengths & Quantum Defects[6]

Alkali	D_1 (Laser) (nm)	D_2 (Pump) (nm)	ΔE ($P_{3/2}$-$P_{1/2}$) (cm^{-1})
Li	670.98	670.96	0.34
Na	589.76	589.10	17.2
K	770.11	766.70	57.7
Rb	794.11	780.25	237
Cs	894.59	852.35	554

As can be seen from Table 1 the difference in energy between the pump and the lasing is extremely small which leads to high SO relaxation rates and theoretical efficiencies. The heavier alkalis show a larger difference in the pump and laser wavelength giving a slightly lower SO relaxation rate and efficiency. In spite of this, the heavier alkalis are generally better DPAL gain media because of the line width of the pump source. Since most diodes are quite broadband, it is important to use a gain medium that has a large separation between D_1 and D_2 so that only the $^2P_{3/2}$ state is pumped. Tables 2-5 below list some relevant characteristics of rubidium and cesium.

Table 2. Rubidium D_2 Transition Optical Properties[8]

Property	Symbol	Value
Frequency	ν_0	384.2304844685(62) THz
Energy	$h\nu_0$	1.589049462(38) eV
Wavelength	λ	780.241209686(13) nm
Lifetime	τ	26.2348(77) ns
Decay Rate	Γ	$38.117(11) \times 10^6$ s^{-1}
Natural Line Width (FWHM)		6.0666(18) MHz
Absorption Oscillator Strength	f	0.695 77(29)

Table 3. Rubidium D_1 Transition Optical Properties[8]

Property	Symbol	Value
Frequency	ν_0	377.107463380(11) THz
Energy	$h\nu_0$	1.559591016(38) eV
Wavelength	λ	794.978851156(23) nm
Lifetime	τ	27.679(27) ns
Decay Rate	Γ	36.129(35)× 10^6 s^{-1}
Natural Line Width (FWHM)		5.7500(56) MHz
Absorption Oscillator Strength	f	0.342 31(97)

Table 4. Cesium D_2 Transition Optical Properties[9]

Property	Symbol	Value
Frequency	ν_0	351.72571850(11) THz
Energy	$h\nu_0$	1.454620563(35) eV
Wavelength	λ	852.34727582(27) nm
Lifetime	τ	30.405(77) ns
Decay Rate	Γ	32.889(84)× 10^6 s^{-1}
Natural Line Width (FWHM)		5.234(13) MHz
Absorption Oscillator Strength	f	0.7164(25)

Table 5. Cesium D_1 Transition Optical Properties[9]

Property	Symbol	Value
Frequency	ν_0	335.116048807(41) THz
Energy	$h\nu_0$	1.385928495(34) eV
Wavelength	λ	894.59295986(10) nm
Lifetime	τ	34.791(90) ns
Decay Rate	Γ	28.743(75)× 10^6 s^{-1}
Natural Line Width (FWHM)		4.575(12) MHz
Absorption Oscillator Strength	f	0.3449(26)

In addition to the separation of the D_1 and D_2 lines in both rubidium and cesium, which allows for easy pumping of only one transition, their lasing wavelengths are

desirable due to their positions in the atmospheric transmission plot. Figure 2 shows the transmission plot for the atmosphere from 0.4 to 14 microns with favorable transmission for the lasing wavelengths of rubidium and cesium at 0.795 and 0.894 microns respectively.

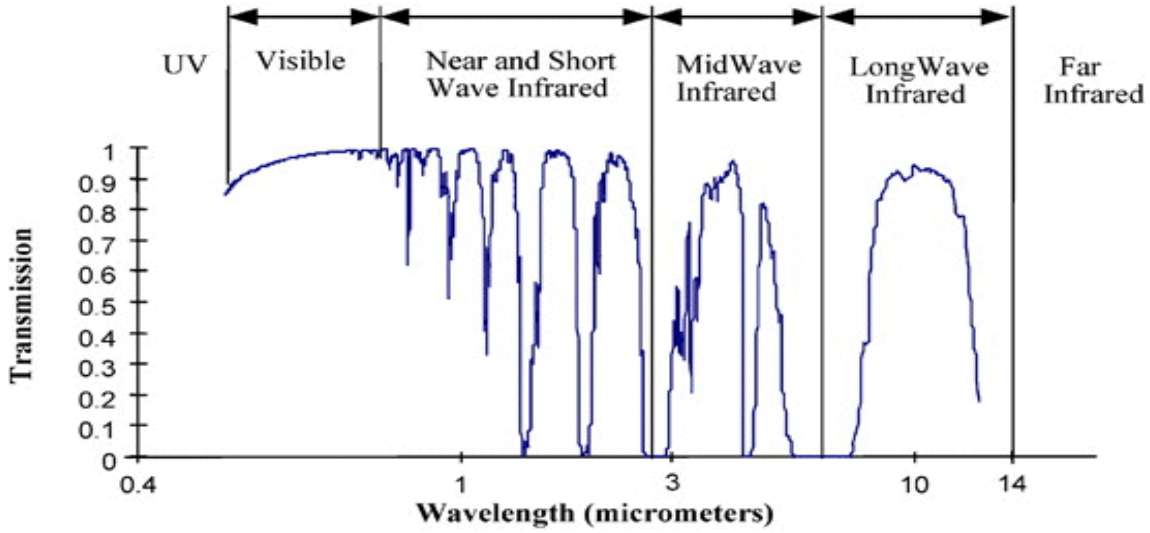

Figure 2. Atmospheric Transmission Window. This diagram shows a high transmission associated with the wavelengths of the alkali lasing transitions.[10]

The relatively low melting points of the alkalis make them easy to handle. In order to be used as a gain medium the alkali needs to be in a vapor form, which necessitates heating. Typical operating temperatures for DPAL systems range from approximately 100 C up to 250 C.[11] By having a low melting point the amount of energy used to create the vapor pressure is minimal. The heating that is a problem in solid state laser systems can actually be a benefit here as the DPAL systems can absorb the excess heat with few, if any, problems.

Though alkalis demonstrate a number of qualities that make them ideal as a gain medium there are some drawbacks to their use. A major drawback is the absorption

profile of the alkali. As was stated earlier the natural linewidth is on the order of hundredths of a GHz or ~10 MHz.[6] This very narrow profile requires either a very narrow pump source and/or profile broadening which is done by adding a buffer gas to homogenously pressure broaden the absorption profile of the alkali. Reactions with water also present a problem that must be overcome in order to use the alkalis. Due to the undesirable reactions, all work with the alkali must be done with sealed cells or done in sealed fume hoods. This also makes broken or damaged cells a problem as the disposal must be carried out in accordance with Occupational Safety and Health Administration (OSHA) guidelines. In spite of these challenges the DPALs concept shows promise.

Gases

In a DPAL system gases are added to the alkali vapor to play one of two roles. The first role is that of a buffer gas that homogenously pressure broadens the absorption profile of the alkali in question. The other role is that of a spin-orbit relaxing or fine-structure mixing gas which is used to quickly bring the excited alkali down from the $^2P_{3/2}$ state to the $^2P_{1/2}$ state.

Helium is typically used to broaden the alkali's absorption line.[5] It is easy to use and its broadening rate of the alkalis rubidium and cesium are known to be approximately 20 MHz/Torr.[6] This allows for the natural linewidth of less than 10 MHz to easily be broadened to the GHz range to match laser diodes without having to go much over an atmosphere of pressure. Other gases display similar broadening characteristics. Table 6 below lists different gases and their broadening abilities for rubidium.

Table 6. Rubidium D_2 Pressure Broadening Coefficients

γ_B (MHz/Torr)

Gas	394 K[0]	320 K[13]	293 K[14,15]	320 K[16]	314.15 K[17]
He	20.0 ± 0.14	15 ± 2	22.5 ± 1.1	18.5 ± 3.3	20.3 ± 0.5
Ne	9.47 ± 0.10	13 ± 3	9.4 ± 0.4	9.8 ± 1.7	
Ar	17.7 ± 0.20	18 ± 2	19.8 ± 0.5	18.5 ± 2.4	
Kr	17.2 ± 0.40	17 ± 2	17.5 ± 1.0	16.2 ± 1.3	
Xe	17.8 ± 0.20	19 ± 2	19.8 ± 0.9	21.2	
H_2	26.4 ± 0.40				
D_2	20.6 ± 0.40				
N_2	18.3 ± 0.40		18.9 ± 0.5		
CH_4	26.2 ± 0.60		26.0 ± 0.7		28.0 ± 0.6
CF_4	17.3 ± 0.60				
C_2H_6					28.1 ± 0.7
C_3H_8					30.5 ± 0.9
C_4H_{10}					31.3 ± 0.9

The second role that gases play in the system is to quickly move the excited alkali down from the $^2P_{3/2}$ state to the $^2P_{1/2}$. This movement needs to be done at a rate much greater than the spontaneous rate out of the $^2P_{3/2}$ in order to produce an efficient system. The spin-orbit relaxing or fine-structure mixing gas accomplishes this. In the first DPAL demonstration by Krupke *et al*. and in subsequent experiments, ethane was used as the SO relaxer.[5] The use of ethane can be problematic. Zhdanov *et al*. observed that ethane in cells with temperatures above 120 C led to black soot on the windows of the cell.[11] This observation has led to the exploration of gases lacking carbon such as ^{4}He and ^{3}He. Various rubidium-gas combinations can be seen in Table 7.

Table 7. Various Rubidium-Gas Collisional Properties

Collision Partner	$\sigma_{P_{1/2}\rightarrow P_{3/2}}$ (10^{-16} cm^2)	$\sigma_{P_{3/2}\rightarrow P_{1/2}}$ (10^{-16} cm^2)	Temp (K)	References
H_2	10.0 ± 1.2	13.9 ± 1.7	330	18
H_2	7 ± 3		340	19
H_2	26 ± 13		1720	19
H_2	>50	>30	1720	20
H_2	11	15	340	21
D_2	21.4 ± 2.6	29.8 ± 3.6	330	18
D_2	22	30	340	21
N_2	13.2 ± 1.6	18.4 ± 2.2	330	18
N_2	10 ± 5		340	19
N_2	20 ± 10		1720	19
N_2	99 ± 20	60 ± 12	1720	20
N_2	16	23	340	21
N_2	<2	7	300	22
O_2	66 ± 33	40 ± 20	1720	20
HD	18	25	340	21
H_2O	120 ± 25	73 ± 15	1720	20
CH_4	29.5 ± 3.5	41.0 ± 5.0	330	18
CH_4		36	340	23
CH_4	30	42	340	21
CF_4	9.5 ± 1.1	13.2 ± 1.6	330	18
CD_4		36	340	23
CD_4	28	38	340	21
CH_2D_2		37	340	23
C_2H_4	23	32	340	21
C_2H_6	57	77	340	21

The fine-structure mixing rate can be calculated using the equation:

$$\gamma_{P_{3/2}\rightarrow P_{1/2}} = n_{gas}\sigma_{P_{3/2}\rightarrow P_{1/2}}v_r \quad (1)$$

where n_{gas} is the number density of the spin orbit relaxing gas, $\sigma_{P_{3/2}\rightarrow P_{1/2}}$ is the collisional cross section given in Table 7 and v_r is the thermally averaged relative velocity given by:

$$v_r = \left[\frac{8k_BT}{\pi}\left(\frac{1}{m_{alkali}} + \frac{1}{m_{gas}}\right)\right]^{1/2} \quad (2)$$

With this equation along with Table 7 it is possible to calculate the mixing rate. In order to be efficient this mixing rate must be much greater than the spontaneous emission rate out of the $^2P_{3/2}$ state so as not to create a bottleneck in the lasing cycle. Though the earlier DPAL demonstrations used two gases to fulfill the roles of the broadening and SO gases it is not necessary to use separate gases. Helium can be used for both the broadening and as the SO relaxer, though it has a smaller collisional cross-section requiring more molecules and more pressure to provide the desired effect.[24,25] Ethane or methane can similarly be used to simultaneously broaden the absorption line while acting as the SO relaxing gas.[11] The use of the either ethane or methane in this capacity will increase the relaxation rate compared to helium while still maintaining approximately the same broadening characteristics as the helium alone.

Power

For a laser system to be useful as a weapon it must have a high power output. Accordingly, the goal of much of the DPAL research is to scale these systems to higher and higher powers. In a DPAL system the output power is dependent upon the efficiency of the system, the number concentration of alkali in the cell, and the amount of spin-orbit relaxing gas present. Additionally in a pulsed system, the number of recycles each alkali atom can make in the period of the pump pulse may become a limiting factor.

In a DPAL the alkali metal must be heated to drive the vapor pressure within the cell. The simple equation that governs this relation between pressure, and therefore concentration of the rubidium vapor in the cell, and temperature is given by[8,9]

$$P_{Rb} = 10^{2.881+4.312-\frac{4040}{T+273}} \tag{3}$$

and for a cesium vapor

$$P_{Cs} = 10^{2.881+4.165-\frac{3830}{T+273}} \tag{4}$$

The temperature used in the equations is in Celsius with the other numbers being variables of the alkali in question. Then using the pressure of the alkali vapor in the cell and the ideal gas law, the number density of alkali in the cell becomes

$$n_{alkali} = \frac{P_{alkali} * 133.322}{k_B * (T + 273)} * \frac{1}{10^6} \tag{5}$$

where k_B is Boltzmann's constant and the units are in number of alkali atoms per cubic cm.

A high SO relaxation rate is necessary for a high power output of a DPAL system. The reason for this is the relaxation rate governs the speed at which an excited alkali is able to move from the $^2P_{3/2}$ state down to the $^2P_{1/2}$ state to lase. If the pumping rate is such that there are many more excited atoms in the $^2P_{3/2}$ state than there are collisional partners then a bottleneck will form. When this bottleneck forms, the output, as a function of input, will begin to roll over until the output power becomes a constant for any greater input power. This effect is seen in both a CW pumped and pulsed system and is the main limiting effect in the CW systems.

As mentioned previously a pulsed system has an extra dependence that involves the pump pulse width. In a pulsed system the ability to excite the alkali atoms is restricted to the short time the pulse is on as opposed to the CW system that is always exciting the alkali within the system. This short pulse means that for high intensities there will be many more photons incident upon the system than number of alkali atoms present. Due to this discrepancy in number of atoms compared to the number of photons each alkali must be reused to absorb the photons. This ability to be reused within a single pulse will be referred to as being recycled. There is a lifetime associated with the length of time it takes each alkali atom to absorb, SO relax, and emit before it can be reused.

By determining the lifetime of the alkali it becomes possible to make an estimate of the number of times the alkali can be recycled in a single pulse. In a DPAL system with a high pump intensity (*i.e.* enough to completely bleach the sample) the lifetime of a single recycle is constant and for the purposes of this experiment dependent only on the SO relaxation rate. The relaxation rate determines the number of atoms that can be moved from the $^2P_{3/2}$ state to the $^2P_{1/2}$ per second. Taking the inverse of this rate the lifetime of the alkali in the excited $^2P_{3/2}$ state is determined. Also, if the intensities are much greater than required to excite all the atoms in the cell, the pumping and lasing processes can be considered negligible compared to the relaxation time from the $^2P_{3/2}$ to $^2P_{1/2}$ states. This leaves only the relaxation time for the recycle lifetime of the alkali.

The pulse width of the pump beam now becomes important. With the finite lifetime of the recycled alkali now determined, it is possible to determine the number of times a single alkali can be used in a pulse. Longer pulses lead to more recycles possible

for the alkali in question. A greater number of alkali recycles through the system leads to more incident photons that can be absorbed and the reemitted as useful DPAL power. This leads to CW systems being highly dependent upon the SO relaxation rate that determines when the bottleneck will occur. Pulsed systems depend upon the SO relaxation rate, just like the CW systems, which determines the recycling lifetime. They also depend upon pump pulse width that determines the number of recycles an alkali can make and the concentration of alkali in the system.

History

Though the concept of using a gas-phase alkali metal as a gain medium that can be pumped by high efficiency diode lasers has been around for some time, the first demonstrated DPAL was built in 2003 by Krupke *et al*.[5] This first DPAL demonstration used a rubidium vapor as the gain medium with helium and ethane as buffer gas and SO relaxation gas respectively.[5] After the first demonstration of the DPAL concept research in the area expanded rapidly. Within less than a year the same group lead by Beach reported on a cesium DPAL device as well as a model for the system.[6] Potassium DPALs were the last of the common alkali devices to be demonstrated and were performed by Zhdanov *et al*. in 2006.[26]

Power scaling of these devices has also been an issue. The first rubidium DPAL demonstrated in 2003 had an output power of about 30 mW.[5] That number rose greatly over the next couple of years. In 2007 Zhdanov and Knize demonstrated a 10 W CW cesium DPAL.[11] This was followed in 2008 by a 17 W CW rubidium laser[27] and a 48 W CW cesium laser.[28] As time goes on the maximum output power of DPAL devices is

expected to rise with this research exploring high intensity pulsed systems to determine way of improving on these demonstrations.

III. Methodology

Experimental Setup

As stated in the introduction, the goal of this research is to investigate rubidium recycling in a system pumped by a short (2-8 ns) pulsed source. Therefore the laboratory setup involves pumping an alkali vapor that has been mixed with a SO relaxing and pressure broadening gas with a pulsed laser and measuring the power output. With this, the efficiency of the system can be examined as the pulse of the pump source is changed both in width and intensity.

The setup used to explore this is shown in Figure 3.

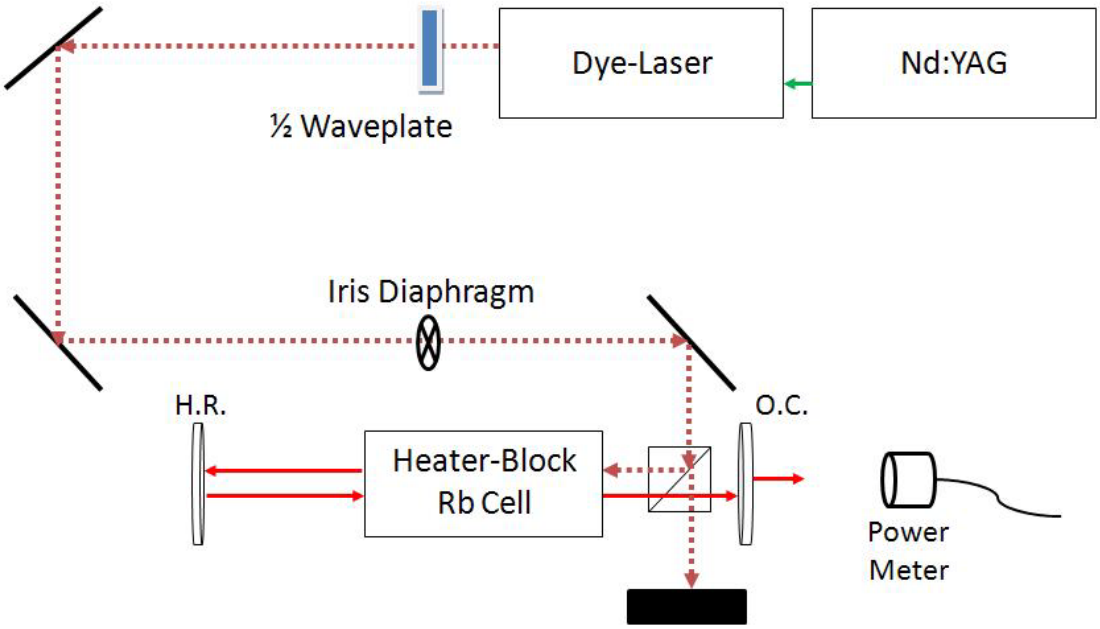

Figure 3. Experimental Setup. The setup includes the pump source consisting of the Nd:YAG and Dye-Laser, steering optics, the laser cavity, and gain media.

There are three main components present in the setup. The components are the pump source and steering apparatus, the laser cavity including the output coupler, and the gain cell itself. Each of the three major sections will be covered in greater detail below.

The pump source starts with a Quanta-Ray Pro Series Pulsed Nd:YAG seed laser. It has a repetition rate of 10 Hz and can output up to 100 mJ per pulse at a wavelength of 532 nm.[29] This output is then used to pump the dye-laser. The dye-laser used in this experiment was a Sirah model PRSC-D-1800 Dye-laser and had a tuning range from about 400 nm to 900 nm using a variety of dyes. For the purposes of this experiment the dye used was LDS765, which allows for tuning from 740-790 nm with the peak intensity at 765 nm. The pump pulse width from this laser changes as power output is changed becoming larger at the higher power levels. Light emitted from the dye-laser was approximately 98% vertically polarized with a 31 GHz spectral linewidth.[30] Once the light has been emitted from the dye-laser it travels through a variety of optical components before entering the cell.

The first optical component is a half waveplate that can be used to rotate the polarization of the pump to the desired orientation. The purpose of adding the waveplate into the system will be discussed further as it pertains to an input power control mechanism. Following the waveplate the beam was steered around the table by a series of mirrors designed for the high energy pulses and then passed through an adjustable aperture iris diaphragm to control beam size. The iris was used to present a uniform beam into the laser cavity and as a means of varying the input beam power and volume without changing input intensity. All of these optical components steer the input beam to

a polarizing beam-splitter within the laser cavity itself which directs the beam towards the end of the cell.

The polarizing beam-splitter and waveplate work in conjunction with each other to control the power going into the cell. Only the vertical polarization of the incoming beam was reflected into the cell. The rest of the beam was sent off into a beam dump. By rotating the waveplate the polarization of the incoming pump beam changed from all vertical polarization to some combination of vertical and horizontal. With the vertical component making up a smaller percentage of the overall power in the beam, a lower power was injected into the DPAL cell.

The next portion of the setup was the laser cavity for the DPAL. A simple linear cavity was constructed around the alkali vapor cell that served as the gain medium as shown above in Figure 3. A 50 cm radius of curvature mirror served as the high reflector of the cavity. The output coupler on the other end of the cavity was flat with a stated reflectivity of 30% and an actual reflectivity of 33% as determined with a photo-spectrometer. The cavity length could be no more than 50 cm to ensure a stable cavity for lasing. An overall cavity length of 42.5 cm was chosen to provide ample room for the gain media while staying well within the stability criteria. The TEM_{00} mode of the cavity along with the collimated pump are shown in Figure 4.

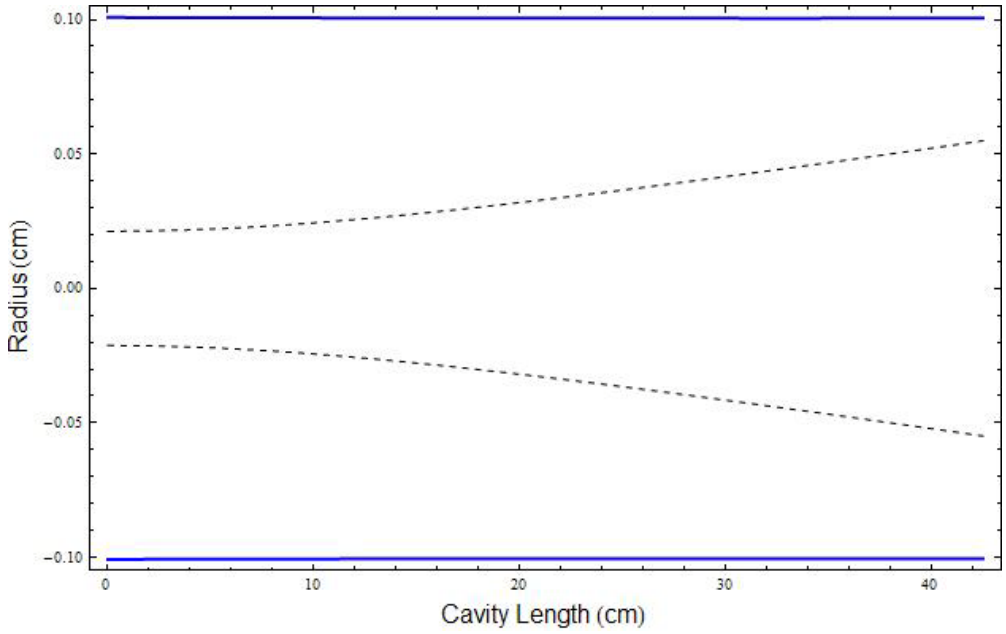

Figure 4. DPAL Cavity Mode Diagram. The solid straight lines show the pump volume while the dashed curved lines show the TEM_{00} mode of the cavity. The DPAL cell was positioned between 16.2 cm and 28.9 cm.

The final portion of the experimental setup is the alkali vapor cell and heater block. The cell that houses both the alkali vapor and the gases is depicted in Figure 5. The cell is 5 inches (12.7 cm) long with a window diameter of approximately one inch (2.54 cm). On the bottom of the main tube is a hot finger that holds the alkali metal and can be heated independently to drive the concentration within the cell. The stem of the cell that connects to the alkali ampoule and the valve is located opposite the hot finger. The ampoule jets off the side of the stem and is created to keep the alkali metal sealed until needed yet still allow for easy transfer to the hot finger. The valve at the top portion of the stem allows for gases to be added into the cell and was sealed during all experiments.

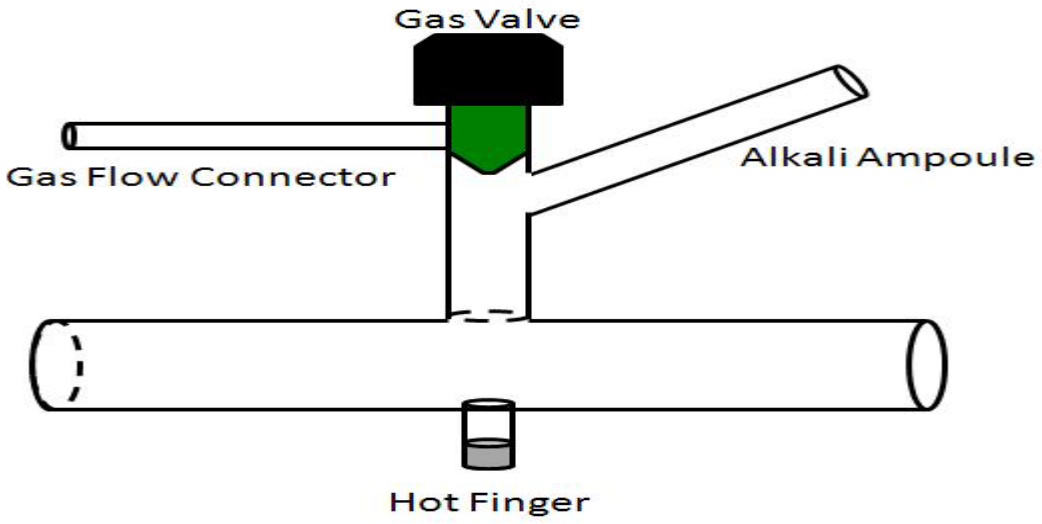

Figure 5. DPAL Cell. Above is a depiction of the alkali cell with main horizontal tube containing alkali vapor and gases with the hot finger below. The structure above the main tube is used for adding the alkali and controlling the gases.

The cell is encompassed by an aluminum heater block. The heater block is designed to heat the cell to both drive the number density of alkali in the system and also to prevent the alkali vapor from condensing on the cell walls. The condensing or plating out of the alkali can cause serious problems if it happens on the windows of the cell. A layer of condensed alkali on the window acts like a highly reflective mirror that prevents pump beam from entering the cell. Therefore the heater block heats the cell and extends a short distance beyond the cell windows to create a pocket of heat. This pocket is necessary to keep the cell windows warm as the heater block cannot touch the windows. The heater block used a Watlow Temperature Controller connected to 10 heater prongs and a thermocouple on a negative feedback loop to control the temperature. Heat tape

along with a separate thermocouple was used around the hot finger to drive the temperature of the alkali and thus the vapor concentration of the alkali inside the cell.

Procedures

The experiment was designed in such a way that multiple parameters could easily be changed to collect the data desired. The different variables that were set and then held constant for the experiment included the temperature of the cell and hot finger, pump beam diameter, and SO/buffer gas pressures. The variable parameters in the experiment were the pump pulse width or the pump pulse power.

Cell preparation was the first step to setting up the experiment. The cell was first pumped by a vacuum pump while heating past the experimental operating temperature. This process removed any impurities from the cell so that the alkali would not be contaminated during the experiment. Following the removal of impurities the cell was sealed and the ampoule containing the alkali was broken releasing the alkali metal into the cell. Once the alkali was added into the cell the system remained completely sealed to avoid any outside contaminants from reacting with the alkali in the system. Immediately after the alkali ampoule was broken the cell was once again hooked up to a vacuum system and pumped down in preparation for the experimental setup.

The next step in setting up the experiment was to add the SO/buffer relaxation gas. With the cell at room temperature, gases were added to the desired pressure and the cell sealed. For this thesis, all work was done using only ethane at 550 ± 10 Torr to both broaden the D_2 absorption line, and to spin-orbit relax the alkali.

Following the insertion of the gas into the system an operating temperature was chosen to be 110 C for the heater-block, which heated the main cell body, and 120 C for the hot finger. The block temperature needed to be high enough, typically within 10 C of the hot finger, that the alkali vapor would not cool and condense out on the cell walls, and more importantly, would not condense on the cell windows. The temperature difference between the heater-block and the hot finger was small to prevent large temperature gradients and condensation.

Data Collection

Data collection consisted of recording the average power of the pump beam going into the cell and the output power of the alkali laser for this input power. The ideal case would have been to measure both the pump power and the output power of the laser simultaneously since the pump power varied somewhat from pulse to pulse. It was possible to determine the percentage sent into the cell and that sent into the beam dump as a function of the wave-plate angle. Using this relationship the pump power was inferred from measurements of the dumped power. This allowed for the simultaneous power measurements of both input power and output power. The power meter used to measure the dump power was ThorLabs model D10MM power meter connected to a ThorLabs digital handheld readout.

The output power of the DPALs cell was collected by placing a detector after the output coupler. The detector used to measure the laser output was a ThorLabs S122B Germanium detector with an operational range of 700-1800 nm and a sensitivity that allowed for detection of powers from 35 nW to 35 mW.[31] A bandpass filter centered at

800 nm with a 10 nm FWHM was placed over this detector to eliminate any of the pump that was not absorbed by the alkali vapor and that passed through the output coupler. During this experiment the fraction of pump beam that was absorbed by the alkali was extremely small and the excess pump would easily overpower the output of the laser at the detector.

The pump pulse profile was measured using scattered light off of the beam dump. This light was passed through a neutral density filter and incident upon a New Focus Visible Nanosecond Photodetector. To record the data from the photodetector, a Wavepro 7100 1-GHz Oscilloscope was used to average 300 pulses or 30 seconds of data. All power measurements were done as 30 second averages as well.

IV. Results and Analysis

Results

One of the major concerns of a DPAL device is its scalability to higher powers. To that end this experiment was designed and set up to determine what effect the pump pulse width and pump power have on the output of the system due to the recycling of the rubidium atoms present inside the cell. The effects of this recycling are explored by varying either the pulse intensity or the pulse width. Figure 6 below shows a representation of the pulsed pump used in the collection of the input power vs. laser output power. For a given pulse width, the input power was varied and laser output power recorded. Some typical input intensity vs. time plots are given in Figure 7. The input power versus output power for the two shortest pulse widths are shown in Figure 8 with all five pulse widths shown in Figure 9.

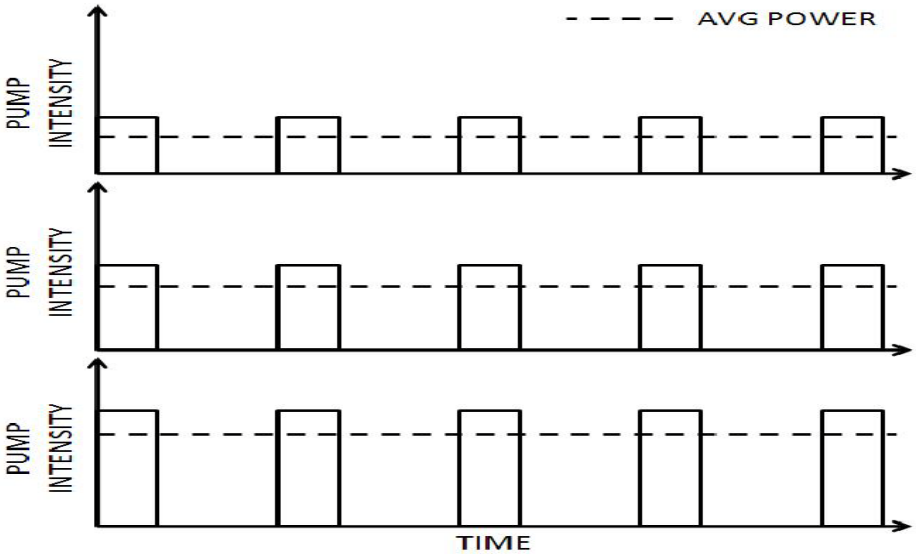

Figure 6. Constant Pulse Width Pump Representation

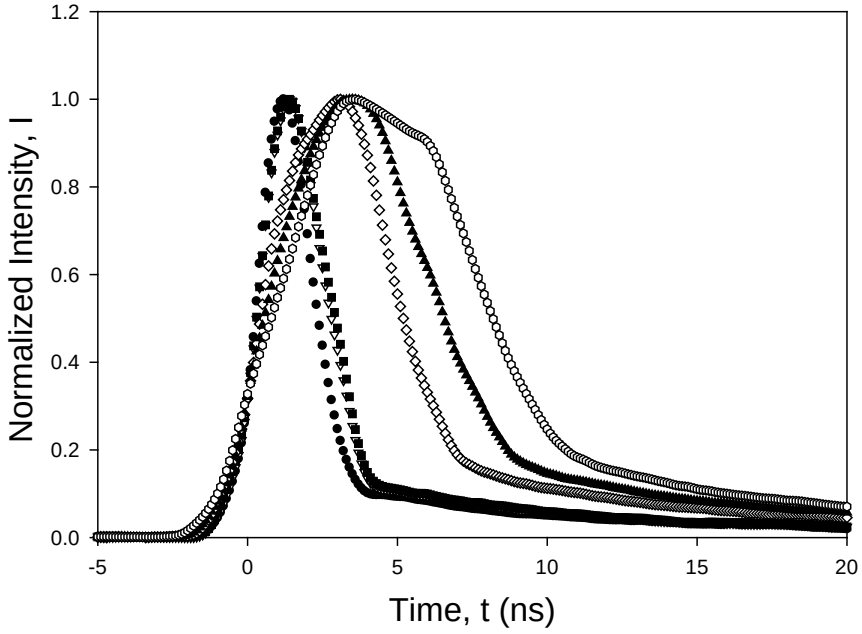

Figure 7. Sample Pump Pulses

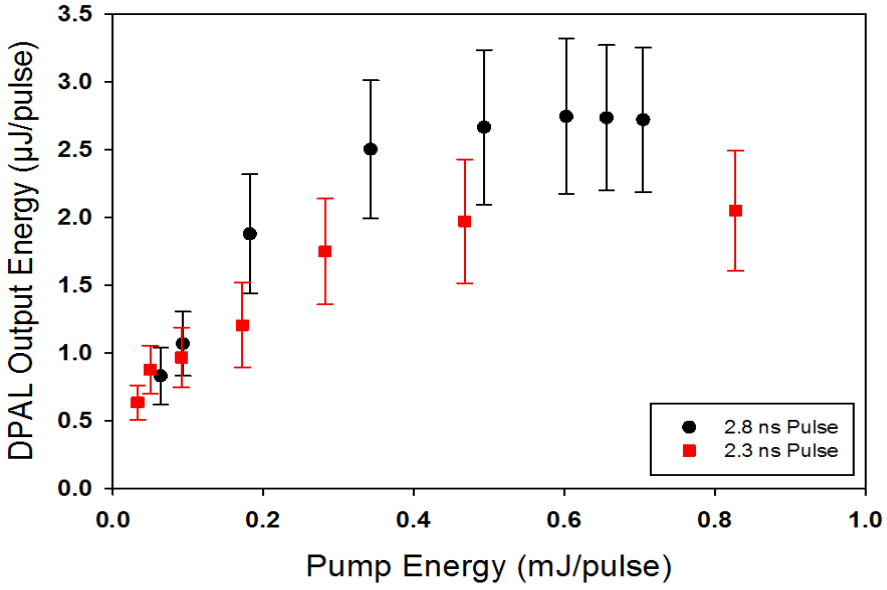

Figure 8. Short Pulse Output Power vs. Input Power. The graph depicts the linear increase in output as a function of the input power up to the asymptotic limit.

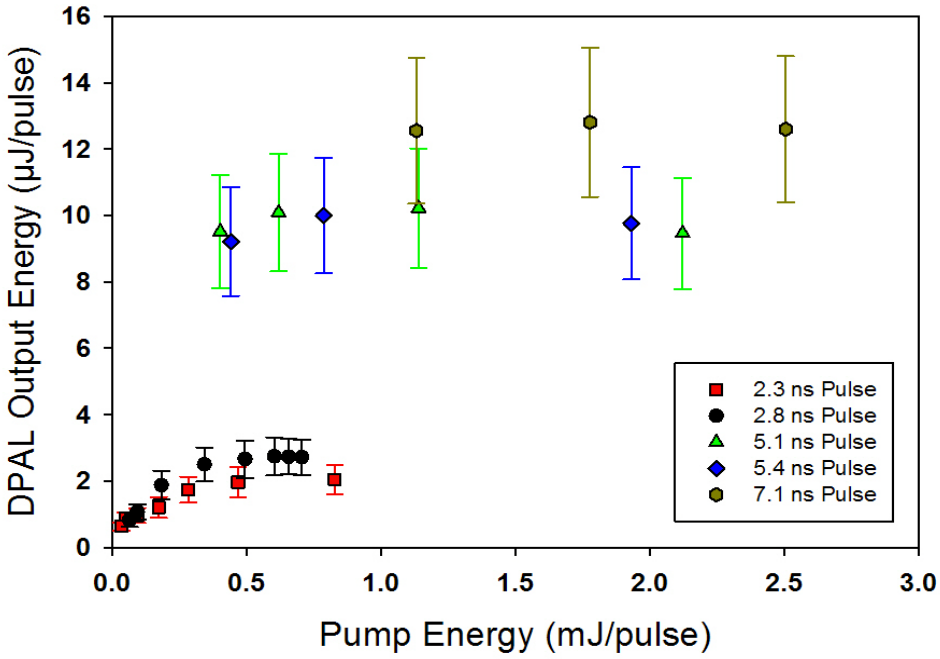

Figure 9. Output Power vs. Input Power. Shows all five of the output power curves for the various pump pulses and their asymptotic limits.

For these data points the cell was filled with 550 ± 10 Torr of ethane to act as both the SO relaxation gas and the pressure broadening buffer gas. The heater block was held at a temperature of 110 C and the hot finger held at 120 C. Using this pressure of ethane and the pressure broadening coefficient of approximately 28.1 MHz/Torr,[11] the FWHM of the $^2S_{1/2}$ to $^2P_{3/2}$ absorption profile is approximately 15.5 GHz at room temperature and then becomes approximately 19.5 GHz as the cell is heated to 110 C. The concentration of rubidium in the cell can be calculated using Equations 3 and 5 and is graphed below as a function of temperature.

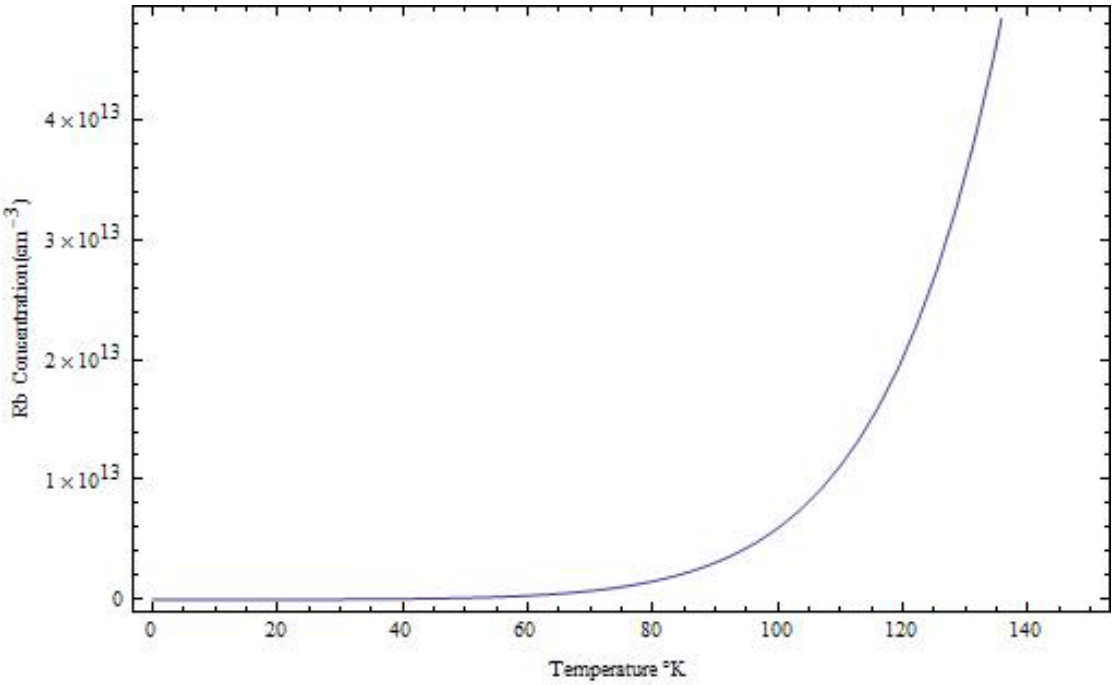

Figure 10. Rubidium Concentration as a Function of Temperature

Using the temperature 120 C, the number density of rubidium atoms inside the cell is 2.01×10^{13} cm^{-3}. Using the pump beam area of 0.0314 cm^2 and the length of the cell there are approximately 8×10^{12} rubidium atoms in the pump volume.

It is apparent from Figures 8 and 9 that an asymptotic power output limit is reached as input power is raised. Figure 8 shows the shorter pulses alone to better display the linear portion that then rolls over into the asymptotic limit while Figure 9 shows all of the data in order to show the relative difference. It is also clear that this asymptotic limit is different for each pump pulse width. A plot of these maximum output powers vs. the pulse width associated with each can be seen below in Figure 11.

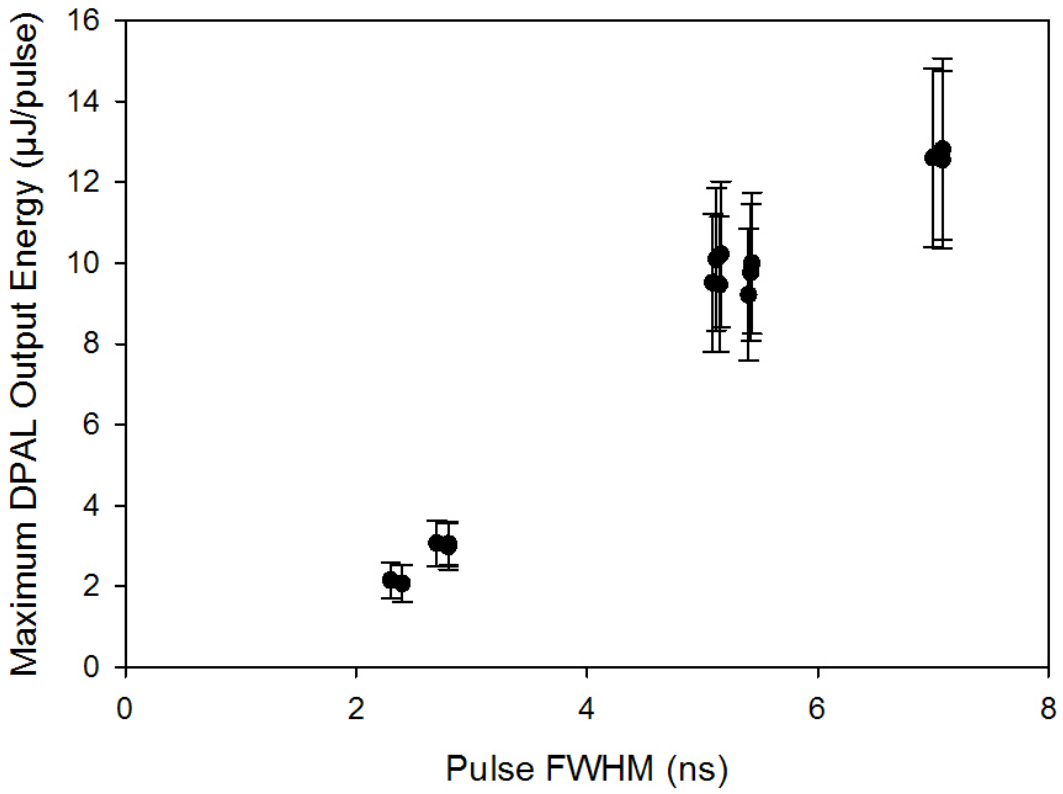

Figure 11. Maximum Output Power vs. Pulse FWHM. The plot shows the linear relation between the maximum output power growing as the FWHM gets larger.

The output vs. input graphs and the max power graph both show a very quantitative view of the pulse width affecting the performance of the laser by showing an increase in maximum output energy with increasing pulse duration. These two graphs show the effects of keeping the pulse width constant for each data set while changing the power going into the system.

A different way to look at this effect is to keep the pump power constant and change the pulse width as shown in Figure 12. Figure 13 shows a set of data that uses the

pump profile shown in Figure 12. The average input power into the cell is constant, but the pulse width and energy are changed simultaneously.

As mentioned previously the pump pulse duration varied as the pump pulse power from the dye-laser was changed. When the pump laser power was set low the pulse duration was short and increased as the dye-laser power was increased. To keep the power into the cell constant while changing the pulse width required the pump laser to be set at an output intensity with corresponding pulse width. The output intensity of the pump was then lowered by using a half waveplate to adjust the degree of polarization followed by a polarizing beam splitter to inject only the vertically polarized component into the cell. In Figure 13 the horizontal axis is in waveplate angle which corresponds to different pulse widths. Higher angles on the waveplate correspond to higher dye-laser output powers to keep the input constant as the higher angles reduce the intensity allowed into the cell. The 0^o mark is where the waveplate axis was aligned with the vertical polarization state of the pump beam from the dye-laser. This allowed most of the pump into the cell. So to keep the power constant the dye-laser pump power is kept low corresponding to a shorter pulse. As the waveplate is rotated to 35^o the percent of pump beam incident upon the cell decreases necessitating an increase in dye-laser pump power and therefore a longer pulse. The data shown is non-linear, as predicted by Malus's law. If the pump pulses were available it is expected that the output power trend would be increasing linearly with pulse duration such as the data shown in Figure 11.

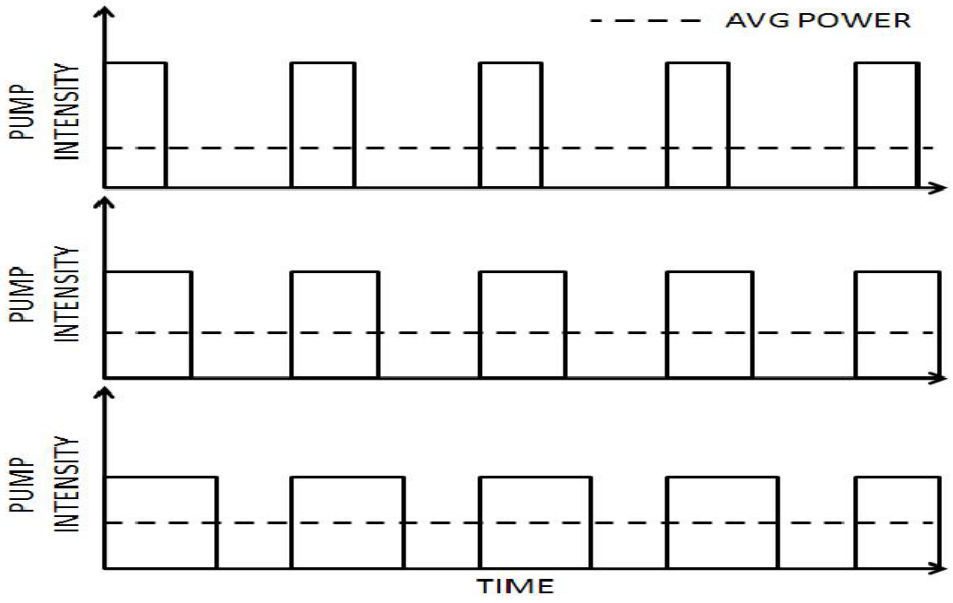

Figure 12. Constant Average Input Power Pump Representation

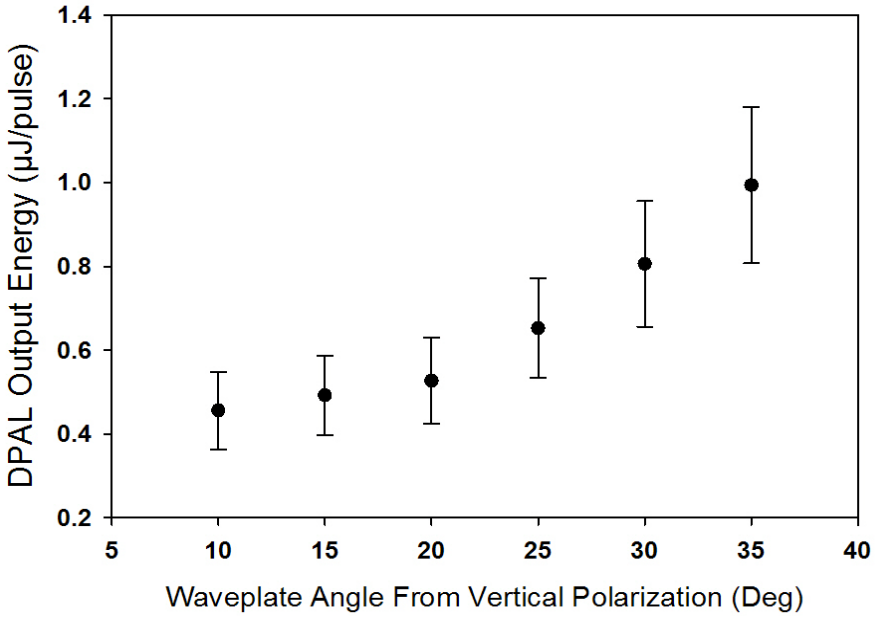

Figure 13. Output Power vs. Waveplate Angle. This graph qualitatively shows how keeping the input into the system constant, at 4.5 mJ/pulse, but changing the pulse width effects performance.

Analysis - Alkali Recycling

Figures 8, 9 and 13 show the power extracted in the form of 795 nm light as a function of the input power going into the cell. Figures 8 and 9 show a quantitative relationship between output power and increasing pulse widths with Figure 13 showing the relationship qualitatively. This relationship is now explained in terms of alkali recycling within the system.

Figure 11 is composed of the data points in Figure 9 that have reached an asymptotic limit. The factor behind this asymptotic limit is believed to be the SO relaxation rate. In the setup described the SO relaxation rate is not high enough to instantaneously move the excited atoms out of the $^2P_{3/2}$ state to the $^2P_{1/2}$ state. This finite lifetime in the excited $^2P_{3/2}$ state eventually leads to a bottleneck effect in which excited alkali atoms cannot be moved down to the $^2P_{1/2}$ state fast enough. When the laser reaches that point of a bottleneck any more input power is wasted as it creates no more power out giving a horizontal line for the slope efficiency.

In both Figure 8 and Figure 9 all of the data sets have hit the asymptotic limit where the SO relaxation rate cannot keep up with the amount of alkali excited. Though each set shows the asymptotic limit, or the maximum power that can be extracted from the cell in the current configuration, the maximum power of each set goes higher as the pulse width of the pump beam gets larger. Figure 11 shows the maximum power of the DPAL output as a function of pump pulse width. In the maximum power vs. pump pulse width graph one would expect a linear relationship between the two parameters with the slope passing through the origin. These two factors are expected due to the simple three-

level system described in Figure 1. Each alkali atom gets excited, spends some amount of time in the $^2P_{3/2}$ state, relaxes and spends some different amount of time in the $^2P_{1/2}$ state, depending on population inversion, before lasing back down to the ground $^2S_{1/2}$ state. After a round trip through the three levels, an alkali atom can be recycled.

To determine the number of times each atom can be recycled in the pump pulse the pulse length is divided by the total time of each round trip. The pump source used inserts over 7.85×10^{14} photons per pulse for the lower power pulse used in the experiment. This compares to the approximately 8.03×10^{12} rubidium atoms present in the volume of the pump beam. Due to the much higher number of photons than rubidium atoms we can assume the $^2S_{1/2}$ state will be quickly depleted to create the population inversion needed for lasing. Using this assumption the time a rubidium atom spends in the ground state before being excited is small and will be considered zero for the purposes of this analysis. Also, the lasing transition ($^2P_{1/2}$ to $^2S_{1/2}$) can be considered to be instantaneous due to the large population inversion. If both the D_1 and D_2 transitions are considered to be so rapid that the time spent in either the $^2S_{1/2}$ or the $^2P_{1/2}$ states is zero, the effective roundtrip time depends only on the time spent in the excited $^2P_{3/2}$ state before relaxing down to the $^2P_{1/2}$ state.

The time spent, or lifetime of the excited rubidium, in the $^2P_{2/3}$ state is simply the inverse of the fine-structure mixing rate. Equations 1 and 2 are used to determine the mixing rate. Some of the important numbers for the equations are the relative velocity, the number density of buffer gas in the cell, and the collisional cross-section for the $^2P_{3/2}$ to $^2P_{1/2}$ transition. The number density of ethane in the cell is calculated using the ideal

gas law with a pressure of 550 Torr of ethane at room temperature to get 1.80×10^{25} m^{-3}. The collisional cross-section for an ethane-Rb is 77×10^{-20} m^2 from Table 7. The third and final quantity needed to determine the spin-orbit relaxation rate is the relative velocity from Equation 2. Inserting the correct temperature in the cell, 110 C, provided by the heater block, and the appropriate masses of rubidium and ethane, the relative velocity is 519.2 m/s. Combining these three numbers gives a SO mixing rate of 7.197×10^9 sec^{-1} or a lifetime of 0.139 ns. Therefore the total time necessary for a rubidium atom to make a complete cycle is 0.139 ± .002 ns.

With the time it takes for a rubidium atom to make one roundtrip in the system now known it is a simple matter to determine the total number to trips made in one pump pulse. The pump pulse FWHM divided by the roundtrip time gives number of trips the alkali makes through the system. Figure 11 from above has been converted from showing the max power out vs. pump pulse FWHM to max power out vs. number of roundtrips made through the system shown below in Figure 14.

The relationship between a longer pulse and the number of round trips is linear leading to the expectation that an increase in the pump pulse width would lead to an increase in the maximum power output of the DPAL device. This relationship is shown experimentally in both Figures 11 and 14. The other expectation was that the linear relationship would pass through the origin or, in other words, that there not be any kind of threshold time requirements, in terms of pulse duration, to create lasing. Clearly visible though is some type of threshold in the data before the lasing begins.

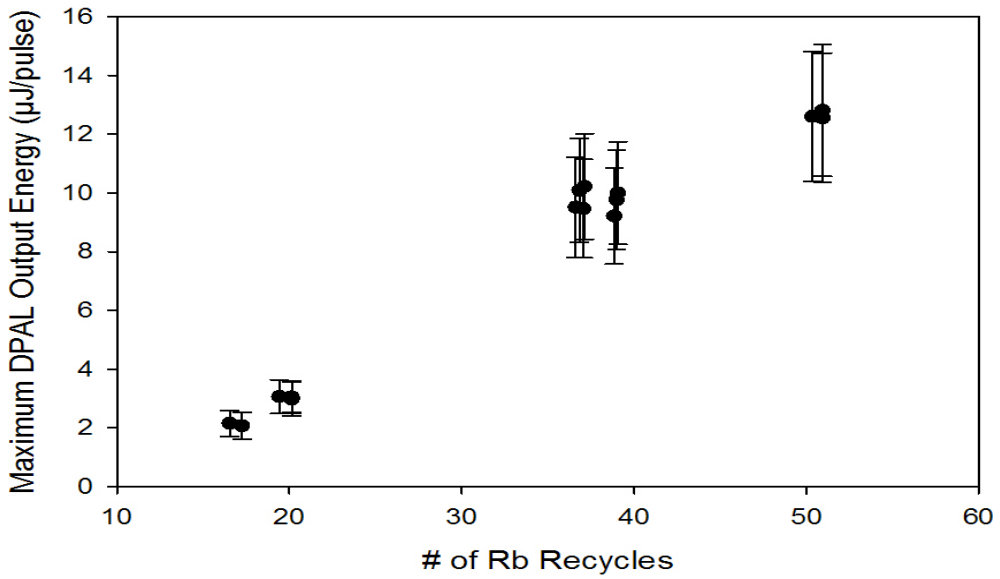

Figure 14. Maximum Output Power vs. # of Recycles. This figure shows how the output power grows in a linear fashion as the rubidium has the ability to be reused more.

The exact cause of the threshold in the data is not completely understood at this point, but there are a few theories on its cause. The first theory is that the simple model developed and described above is correct. In that case the data has an error. The error could be some kind of systematic error that is causing the DPAL output power to register lower than it actually was leading to a negative intercept to the linear relationship as opposed to an intercept of zero or slightly positive. Each of the points would have to be off by a fixed quantity to change the intercept of the line.

On the other hand the data could be completely correct and there is a problem in the understanding of the system. Different variables that were not included in the simple view of the system that might cause this threshold condition range from taking into

account the amount of time the photons take to travel through the cell bleaching the sample to some unaccounted for kinetic process to possible misinterpretation of the data.

The third possibility is that with very short pulses, *i.e.* pulses below the approximately 1 ns threshold that there are not enough photons in the system to meet the conditions of the bottlenecking. This would mean that the number of photons is no longer much greater than the number of rubidium atoms within the cell and therefore the assumptions that the only factor effecting lifetime is the spin-orbit rate would no longer be valid. Whatever the cause of the threshold condition in the data may be, more experimentation is needed to prove or disprove any of these theories.

System Efficiency

As evident from the units on the Input Power vs. Output Power graphs the efficiency of the system was very low. The pump power is measured with units of mW while the output power is reported as uW. For a system that can reach greater than 50 % slope efficiency as demonstrated by multiple papers an efficiency of less than 0.1 % is relatively poor. A few causes for the extremely low slope efficiency of the system are the pump pulse intensity, spectral overlap, and the concentration of excitable rubidium atoms inside the cell.

To determine the spectral overlap of the system both the absorption linewidth of the alkali is needed as well as the spectral FWHM of the pump laser. The absorption linewidth of the alkali is relatively easy to calculate using the pressure broadening coefficient. The number quoted earlier is approximately 28.1 MHz/Torr for ethane with 550 Torr in the system which gives a FWHM of approximately 19.5 GHz for the

rubidium absorption linewidth. To determine the spectral overlap of the system, this linewidth is compared to the linewidth of the pump source. In order to determine the linewidth of the pump source PhD candidates Major Cliff Sulham and Greg Pitz used an un-broadened rubidium sample, which is being considered as a delta function, and interrogated it with the pump source scanning over a range of wavelengths. A blue spot appeared at a pump wavelength of 778.1440 nm and then turned off as the pump scanned past the 778.2080 nm point.[32] This was not the normal $^2S_{1/2}$ to $^2P_{3/2}$ transition but a different transition that is being researched for creating a blue DPAL, however the scan shows where the un-broadened rubidium line starts absorbing the pump and where it stops absorbing. Using the range of pumping wavelengths discussed here the linewidth of the pump source is approximately 31 GHz.

As mentioned earlier there is a significant difference in the number of rubidium atoms available to be excited to the high number of photons incident upon the system. At the lower pump powers (2 mW) there are around a factor of 100 times more photons than there are rubidium atoms in the same volume. Even while accounting for the ability of the alkali atoms to be recycled many times in the length of this incoming pulse there are still many times more photons. Most of these photons are not absorbed on the first pass through the cell or on the return trip from the high reflector. After the pulse has passed through the cell and returned from the high reflector most of the remaining photons are lost through the output coupler with a reflectivity of only 33%. This waste of many of the pump photons has a strong role in the very low slope efficiency observed.

In order to increase the slope efficiency of the system a few things could be done. The first is a closer matching of the pump to the absorption profile of the rubidium $^2S_{1/2}$ to $^2P_{3/2}$ transition. This can only go so far though as it would require inserting a specific amount of buffer gas into the system which might not be what a particular experiment calls for, therefore this is only of limited help. The more effective measure would be to increase the number of rubidium atoms inside the pump volume to absorb the incoming photons. Since the number density of alkali in the system is dependent upon temperature the temperature could be increased to a point. As mentioned earlier in the background black soot starts to form on the windows of the cell degrading performance once the cell is taken beyond a certain temperature. The last of the simple measures that could be taken could be to insert a lens into the system that would expand the collimated beam in order to lower the intensity and pump a larger volume with the same number of photons. Another option would be to lower the power of the pump beam to run in a regime where there are not as many photons per rubidium atom in the cell. This may work with other systems, but with the pump source used in this experiment the intensity is too high and cannot be made low enough to accomplish this.

V. Conclusions and Recommendations

Conclusions of Research

This research into the basic properties of a DPAL system has revealed the importance of kinetic processes in a pulsed configuration. Previous research into CW or quasi-CW DPAL systems has not employed the high intensities present in this experiment. CW systems typically reuse the available alkali atoms so many times that all of the incoming photons are absorbed if they are spectrally matched. In a pulsed system this is no longer the case as the finite amount of time spent in the excited $^2P_{3/2}$ state has to be compared to the width of the pulse coming through to excited said atoms.

This work has observed that the longer pump pulses allow for more power to be extracted from the system. This is due to a single alkali atom being reused many more times for a longer pulse than they are for a shorter pulse. In the setup used for this experiment the roundtrip time for a single rubidium atom was 0.139 ns. The pulses used to pump the system ranged from 2.3 ns to 7.1 ns allowing for a range of 16 to 51 recycles in a single short pulse. This number gets very large when the system is either pumped in much longer pulses and is considered to be infinity when the system moves from a pulsed to a CW system.

While using a pulsed system, the number of alkali present must now be accounted for more carefully and factored into the pump powers needed for the pulse width used. This will lead to more efficient pulsed systems that will allow for much higher intensities. The higher intensities are useful to move the slope efficiencies data out many times past

the threshold point in order to explorer any non-linear effects or breaking points in the laser that will affect the scaling of DPAL systems.

Though this research was done in a low efficiency regime many of the factors that led to the low efficiency can be overcome to boost the system back into the 10%-50% efficiency range demonstrated.[28] With higher efficiencies the level of pump intensities used demonstrate the ability of a DPAL system to be scaled up. This scaling is possible due to the lack of second order processes observed while pumping the system many 100s of times above threshold. In order to take advantage of this, the pump area would need to be increased while keeping the intensity used and the rep rate of the pump would have to be increased greatly. By scaling the system heat load on axis of the pump beam may begin to degrade the system performance or lead to higher order effects that limit the output of the laser, though none of those effects were observed in this experiment.

Recommendations for Future Research

Future research should be focused on exploring pulsed systems further and specifically the alkali recycling problems. A few areas that should be explored include changing the SO relaxation gas concentration, exploring a larger dynamic range in pump pulse widths, and varying the temperature of the DPAL cell.

A SO relaxation gas concentration experiment should also be set up to explore the recycling characteristics of the system using various gas pressures and multiple gases. This would allow for the changing of the effective recycling lifetime of a single alkali atom in the system. By determining this relationship a database could then be made of

various alkali-gas combinations that would allow for the best choices to be made when selecting the alkali and gases for a particular system.

The greater range in pump pulse widths experiment would be identical, but would allow an experimenter to increase the pulse duration to determine if this relationship between maximum output energy per pulse and pump pulse duration continues to be linear. The data presented here look very linear, but might change further out just as a DPAL input seems very linear at lower powers and then rolls over. Even if there is no roll over and the relationship remains linear, just having that knowledge could prove useful.

The last area recommended for research is the temperature of the system and therefore the concentration of alkali. With greater alkali numbers in the system the dependence of the recycling time on the output of the system might change as there are more atoms to absorb the incoming photons. This would be an excellent experiment to combine with the SO relaxation gas changing one at a time.

Bibliography

1. Boeing - Airborne Laser (ABL). *Boeing Defense, Space & Security.* http://www.boeing.com/defense-space/military/abl/index.html.

2. Boeing - Direct Energy Systems (DES). *Boeing Defense, Space & Security.* http://www.boeing.com/defense-space/ic/des/index.html.

3. Glen P. Perram, Salvatore J. Cusumano, Robert L. Hengehold, and Steven T. Fiorino. An Introduction to Laser Weapon Systems. 2010

4. Joint High Power Solid-State Laser (JHPSSL) Program. *Northrop Grumman Aerospace Systems.* http://www.as.northropgrumman.com/products/joint_hi_power/index.html.

5. W. F. Krupke, R. J. Beach, V. K. Kanz, and S. A. Payne. Resonance transition 795-nm rubidium laser. *Optics Letters*, 28: 2336 - 2338, 2003.

6. Raymond J. Beach, William F. Krupke, V. Keith Kanz, and Stephen A. Payne. End-pumped continuous-wave alkali vapor lasers: experiment, model and power scaling. *J. Opt. Soc. AM. B*, 21:2151-2163, 2004.

7. Z. Konefal. Observation of collision induced processes in rubidium-ethane vapour. *Optics Communications* 164:95-105, 1999.

8. Daniel A. Steck. Rubidium 87 D line data. Technical report, http://steck.us/alkalidata, 12 August 2009. Version 2.1.2.

9. Daniel A. Steck. Cesium D line data. Technical report, http://steck.us/alkalidata, 12 August 2009. Version 2.1.2.

10. Keith Krapels. Infared Imaging Systems. *Encyclopedia of Optical Engineering*, 901, 2003.

11. Boris Zhadanov and R. J. Knize. Diode-pumped 10 W continuous wave cesium laser. *Optics Letters*, 32:2167-2169, 2007.

12. Matthew D. Rotondaro and Glen P. Perram. Collisional broadening and shift of the rubidium D_1 and D_2 lines ($5^2S_{1/2} \rightarrow 5^2P_{1/2}, 5^2P_{3/2}$) by rare gases, H_2, D_2, N_2, CH_4 and CF_4. *J. Quant. Spectrosc. Radiat. Transfer* Vol 57, 4:497-507, 1997.

13. S. L. Izotova, A. I. Kantserov, and M. S. Frish, *Opt. Spectrosc.* 51:107, 1981.

14. P. Ya. Kantor and L. N. Shabanova, *Opt. Spectrosc.* 58:614, 1985.

15. V. N. Belov, Opt. Spectrosc. 51:22, 1981.

16. C. Ottinger, R. Scheps, G. W. York, and A. Gallagher, *Physical Review A* 11:1815, 1975.

17. Nathan D. Zameroski, Wolfgang Rudolph, Gordon D. Hager and David A. Hostutler. Pressure broadening and collisional shift of Rb by CH_4, C_2H_6, C_3H_8, n-C_4H_{10}, and He. Preprint copy.

18. Matthew D. Rotondaro and Glen P. Perram. Role of rotational-energy defect in collisional transfer between the 52P1/2,3/2 levels in rudidium. *Physical Review A* 57:4045-4048, 1998.

19. J. M. Mestdagh, P. de Pujo, J. Cuvellier, A. Binet, P. R. Fournier, and J. Berlande. *J. Phys. B* 15:663, 1982.

20. P. L. Lijnse, P. J. Th. Zeegers, and C. Th. J. Alkemade, J. Quant. *Spectrosc. Radiat. Transf.* 13:1033, 1973.

21. E. S. Hrysyshyn and L. Krause. *Can. J. Phys* 48:2761, 1970.

22. J. A. Bellisio, P. Davidovits, and P. J. Kindlmann. *J. Chem. Phys*. 48:2376, 1968.

23. R. A. Phaneuf and L. Krause. *Can J. Phys*. 58:1047, 1980.

24. Sheldon S.Q. Wu, Thomas F. Soules, Ralph H. Page, Scott C. Mitchell, V. Keith Kanz, and Raymond J. Beach. Resonance transition 795-nm rubidium laser using 3He buffer gas. *Optics Communications* 281:1222-1225, 2007.

25. Sheldon S.Q. Wu, Thomas F. Soules, Ralph H. Page, Scott C. Mitchell, V. Keith Kanz, and Raymond J. Beach. Hydrocarbon-free resonance transition 795-nm rubidium laser. *Optics Letters* Vol 32, No 16, 2007.

26. B. Zhdanov, C. Maes, T. Ehrenreich, A. Havko, N. Koval, T. Meeker, B. Worker, B. Flusche, R.J. Knize. Optically pumped potassium laser. *Optics Communications* 270:353-355, 2007.

27. B.V. Zhdanov, A. Stooke, G. Boyadjian, A. Voci, and R.J. Knize. 17 Watts Continuous Wave Rubidium Laser. *OSA/CLEO/QELS*, 2008.

28. B.V. Zhdanov, J. Sell, and R.J. Knize. Multiple laser diode array pumped Cs laser with 48 W output power. *Electronics Letters* Vol. 44 No. 9, 2008.

29. Newport. Quanta-Ray Nd-YAG Laser Family. Technical Report, http://www.newport.com/images/webDocuments-EN/images/14773.pdf

30. Newport. Pulsed Dye Laser Series. Technical Report, http://www.newport.com/images/webDocuments-EN/images/11810.pdf

31. Thorlabs. Spec Sheet: S122B Germainium Power Meter Optical Head. Doc 13337-S01 Revision B, 2006.

32. Cliff Sulham. Ph.D. Canidate, Air Force Institute of Technology, WPAFB Ohio, Personal Correspondence. 2010.

Vita

Second Lieutenant Wooddy S. Miller graduated from Lakeside Central High School in Trenton, Nebraska. He entered undergraduate studies at the United States Air Force Academy in Colorado Springs, Colorado where he graduated with a Bachelor of Science degree in Physics in May 2008. He was commissioned through the Air Force Academy.

His first assignment was at Wright-Patterson Air Force Base, Ohio as a student at the Air Force Institute of Technology in August 2008. Upon graduation, he will be assigned to the Air Force Research Laboratory's, Sensors Directorate at Wright-Patterson Air Force Base.

REPORT DOCUMENTATION PAGE

Form Approved
OMB No. 074-0188

1. REPORT DATE *(DD-MM-YYYY)*	2. REPORT TYPE	3. DATES COVERED *(From – To)*
25-03-2010	Master's Thesis	January 2009 – March 2010

4. TITLE AND SUBTITLE

Rubidium Recycling in a High Intensity Short Duration Pulsed Alkali Laser

5a. CONTRACT NUMBER In-House

5b. GRANT NUMBER

5c. PROGRAM ELEMENT NUMBER

6. AUTHOR(S)

Miller, Wooddy S., Second Lieutenant, USAF

5d. PROJECT NUMBER

5e. TASK NUMBER

5f. WORK UNIT NUMBER

7. PERFORMING ORGANIZATION NAMES(S) AND ADDRESS(S)

Air Force Institute of Technology
Graduate School of Engineering and Management (AFIT/EN)
2950 Hobson Way, Building 640
WPAFB OH 45433-8865

8. PERFORMING ORGANIZATION REPORT NUMBER

AFIT/GAP/ENP/10-M11

9. SPONSORING/MONITORING AGENCY NAME(S) AND ADDRESS(ES)

HEL-JTO
901 University Blvd SE Ste 100
Albuquerque NM 87106
505-248-8200, hel-jto@jto.hpc.mil

10. SPONSOR/MONITOR'S ACRONYM(S)
HEL-JTO

11. SPONSOR/MONITOR'S REPORT NUMBER(S)

12. DISTRIBUTION/AVAILABILITY STATEMENT

APPROVED FOR PUBLIC RELEASE; DISTRIBUTION UNLIMITED.

13. SUPPLEMENTARY NOTES

14. ABSTRACT

Laser induced fluorescence was used to study how pump pulse duration and alkali recycle time effects maximum power output in a Diode Pumped Alkali Laser (DPAL) system. A high intensity short pulsed pump source was used to excited rubidium atoms inside a DPAL-type laser. The maximum output power of the laser showed a strong dependence upon the temporal width of the pump pulse in addition to the input pump intensity. A linear relationship was observed between the maximum output power and the pulse width due to the effective lifetime of the excited state, defined as the time it takes for the alkali to be excited to the $^2P_{3/2}$, relax down to the $^2P_{1/2}$ state, and finally lase. This effective lifetime, calculated to be 0.139 ns, allowed for a calculation of the number of times each alkali atom in the pump volume could be used for lasing during a pulse. The number of recycles ranged from approximately 15 during the shorter 2 ns pulses up to 50+ times during the 7-8 ns pulses. The maximum output of the system scaled linearly with the number of cycles available.

15. SUBJECT TERMS

DPAL, Alkali Laser, Rubidium, Pulsed

16. SECURITY CLASSIFICATION OF:			17. LIMITATION OF ABSTRACT	18. NUMBER OF PAGES	19a. NAME OF RESPONSIBLE PERSON
a. REPORT	b. ABSTRACT	c. THIS PAGE			Jeremy C. Holtgrave, Lt Col, USAF
U	U	U	UU	56	19b. TELEPHONE NUMBER *(Include area code)* (937) 785-3636, ext 4649 (Jeremy.Holtgrave@afit.edu)

Standard Form 298 (Rev. 8-98)
Prescribed by ANSI Std. Z39-18